Journal of the European Ceramic Society 7 (1991) 49–54

Acoustic Emission Characteristics and Fracture Toughness of Artificial Graphite Electrodes

Naotaka Ekinaga

Fuji Research Laboratory, Tokai Carbon Co., Ltd, 394-1, Oyama-cho, Sunto-gun, Shizuoka-ken, 410-14 Japan

Kinji Tamagawa & Hideaki Takahashi

Research Institute for Strength and Fracture of Materials, Faculty of Engineering, Tohoku University, Aza-aoba, Aramaki, Sendai-shi, Miyagi-ken, 980 Japan

(Received 13 March 1990; accepted 20 September 1990)

Abstract

The acoustic emission (AE) method was applied to monitor the initiation of macroscopic and microscopic cracks in three artificial graphite electrodes under three-point bending by using notched specimens. AE signals detected by piezoelectric transducer were classified into eight levels of amplitude. The load–displacement curves on three samples show non-linear behaviour. Low-level AE signals are detected from the early stage of loading. On the other hand, high-level AE signals above 2·0 V are detected around the maximum load. The sample with high Young's modulus gives late initiation of AE signals, but a large number of the signals at each AE level. The J-values determined from the abrupt increase in cumulative AE energy, J_{iAE}, are considered to correspond to the critical value J_{IC} for the initiation of macroscopic crack; 0·0135, 0·0155 and 0·0165 kg/mm being determined on three samples. The load corresponding to the J_{iAE}-value is in the range of 85 to 90% of the maximum load. The crack-opening displacement corresponding to J_{iAE}-value shows a similar value and does not coincide in position with maximum load on each sample. The AE signal generating model on porous artificial graphite electrode is also discussed.

Die Bildung makroskopischer und mikroskopischer Risse dreier Graphitelektrodenwerkstoffe wurde im Dreipunktbiegeversuch an gekerbten Proben in Verbindung mit der Schallemissionsmethode (acoustic emission, AE) untersucht. Die AE-Signale der piezoelektrischen Wandler wurden in acht Intensitätsstufen unterteilt. Die Belastungs–Durchbiegungs-Kurven dreier Proben zeigten ein nicht lineares Verhalten. Während der Anfangsphase der Belastung wurden nur AE-Signale geringer Intensität empfangen. Andererseits wurden im Bereich der höchsten Belastung hohe AE-Signale über 2·0 V gemessen. Proben mit einem hohen E-Modul geben erst spät AE-Signale aber eine hohe Anzahl auf jeder Intensitätsstufe. Es wird angenommen, daß J-Werte, die aus dem spontanen Ansteigen der AE-Energie-Summenkurve abgeleitet wurden, J_{iAE}, mit dem kritischen J_{IC}-Wert zur Bildung makroskopischer Risse in Zusammenhang stehen; an drei Proben wurde 0·0135, 0·0155 und 0·0165 kg/mm gemessen. Die dem J_{iAE}-Wert entsprechende Belastung liegt bei circa 85–90% der maximalen Belastung. Auch die Durchbiegung bei Erreichen des J_{iAE}-Wertes zeigt einen ähnlichen Wert und stimmt nicht mit der Durchbiegung bei maximaler Probenbelastung überein. Eine Modellvorstellung zur Erzeugung der AE-Signale in porösen Graphitelektroden wird ebenso diskutiert.

On a appliqué la méthode d'émission acoustique (AE) à l'étude de l'initiation des fissures macroscopiques et microscopiques dans trois électrodes de graphite artificiel en flexion 3 points sur des échantillons entaillés. Les signaux AE détectés à l'aide d'un transducteur piezoélectrique étaient classés en huit niveaux d'amplitude. Les courbes charge–déplacement des trois éprouvettes montrent un comportement non linéaire. Des signaux AE de faible niveau sont détectés à partir de l'étape de charge initiale. Des signaux AE de niveau élevé (supérieurs à 2·0 V) sont d'autre part détectés au voisinage de la charge

Journal of the European Ceramic Society 0955-2219/91/$3.50

maximale. L'échantillon possédant un module de Young élevé présente une initiation tardive des signaux mais un grand nombre de signaux à tous les niveaux d'AE. Les valeurs de J déterminées à partir de l'accroissement brutal de l'énergie cumulative d'AE, J_{iAE}, sont assimilées à la valeur critique J_{IC} pour l'initiation des fissures macroscopiques; 0·0135, 0·0155, 0·0165 kg/mm pour les trois échantillons. La charge correspondant à la valeur J_{iAE} est comprise entre 85 et 90% de la charge maximale. Le déplacement d'ouverture de fissure correspondant à J_{iAE} a une valeur similaire et ne coincide pas en position avec la charge maximale sur chacun des échantillons. On discute également d'un modèle générateur des signaux AE pour l'électrode poreuse de graphite artificiel.

1 Introduction

Artificial graphite electrodes have been in use as terminals in electric arc furnaces for steel making. In this usage, the fracture by thermal shock occurs at the tip of the electrode and causes large amounts of reductions in operations. Therefore, various efforts in science and technology have been devoted to the improvement of the thermal shock resistance of the electrodes and to its evaluation. It is still necessary, however, to perform basic and precise research on the fracture behavior of such a porous material. The authors previously applied electrical potential measurement to monitor the crack extension with loading in three-point bending fracture toughness tests and reported the relation between fracture toughness and crack extension.[1] On artificial graphite electrodes, the generation of several microcracks around the notch tip was observed before extension of the main crack. The formation of microcracks results in an increase in electrical potential, and consequently made it difficult to determine accurately the initiation of the crack, which would lead to fracture of the specimen from the notch tip, by the electrical potential method.

Recently, the acoustic emission (AE) method has been utilized to monitor the microscopic and macroscopic crack initiation in various materials and has been shown to be a powerful tool for the study of localized microscopic cracking behavior.[2,3] The purpose of this experiment is the accurate determination of macroscopic crack initiation and J_{IC}-values of artificial graphite electrodes. For this requirement, the AE method was applied to determine the macroscopic crack initiation of artificial graphite electrodes in three-point bending fracture toughness tests. In addition, the relation between J_{IC} and Young's modulus, and the AE signal-generating model of artificial graphite electrodes were discussed.

2 Experimental

2.1 Test specimens

The artificial graphite electrode is composed of two parts, pole and nipple, both of which are produced by mixing coke particles with binder pitch, extruding, baking and then graphitizing at 3000°C. The pole and nipple parts of the electrode are usually made by using cokes of large grain sizes above several millimeters in order to have thermal shock resistance. As a consequence of being large, the coke grains have various pores, which lead to complex crack propagation and fracture behavior.

In this experiment, three samples, A and B being the pole part and C the nipple part of artificial graphite electrodes, were selected; their properties are summarized in Table 1. These were commercially produced in the plant of Tokai Carbon Co. Maximum grain sizes of the samples A and B were about 10 mm, but that of the sample C was less than 10 mm. The petroleum coke particles with suitable size distribution were kneaded with coal-tar pitch, extruded to the size of 50·8 cm (20 in) diameter with 2 m length in the samples A and B and to 25·4 cm × 2 m in sample C, baked at 1000°C and graphitized at 3000°C. The samples B and C were impregnated with pitch after baking. The ash contents of the three samples were less than 0·2%. Specimens with height

Table 1. Properties of the graphite electrodes used

Electrode	*Bulk density* (g/cm^3)	*Specific resistance* ($\times 10^{-4}\,\Omega\,cm$)	*Young's modulus* (kgf/mm^2)	*Transverse strength* (kgf/cm^2)	*CTE*[a] ($\times 10^{-6}\,°C$)
A	1·65	6·7	860	108	0·40
B	1·68	5·3	1070	138	0·26
C	1·83	3·3	2140	311	0·02

[a] CTE = Coefficient of thermal expansion from RT to 100°C.

and width each of 40 mm and the length of 200 mm were cut from these electrodes, the long direction being parallel to extrusion. A notch with the depth of 20 mm (50% of the height of the specimen) was introduced by a diamond cutter, vertical to the extruding direction. The radius of the notch tip was 0·2 mm.

2.2 Fracture test

Three-point bending tests were carried out by an autograph (IS-500, Shimadzu, Kyoto, Japan) with a cross-head down speed of 0·1 mm/min at room temperature. The measurement set-up is shown in Fig. 1 as a block diagram. In order to measure the crack-opening displacement (COD), a clip gage was mounted between two jigs which were fixed at two sides of the notch. The load point displacement for J-value calculation was also measured during loading by using another clip gage which was set up on the surface of the specimen. For the bending test, the J-integral was calculated by using the following equation:[4]

$$J = \frac{2A}{Bb}$$

where A is the area under the load–load point displacement curve, B the depth of the specimen and b the length of the ligament.

In order to monitor the initiation and extension of macroscopic cracks, a crack gage (KV-5B, 0·2 mm pitch, Kyowa Dengyo, Tokyo, Japan) was attached in front of the notch tip on the side surface of the specimen.

2.3 AE monitoring system

The AE analysis system (Cracking Monitor, MD-1100SS, San Denshi, Tokyo, Japan) and the location of the AE sensor are also shown in Fig. 1. Stress waves emitted from the notch tip were monitored by piezoelectric transducer (AE-905S, NF Corporation, Tokyo, Japan), which is a broad-band type

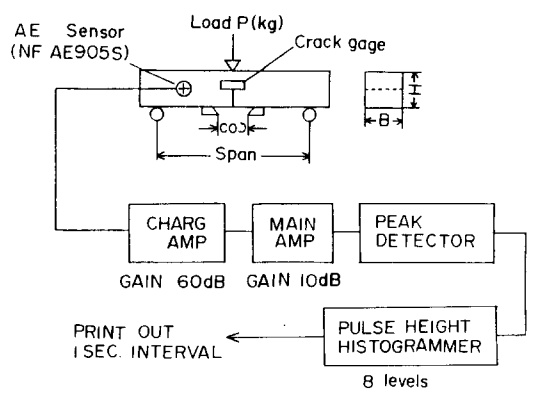

Fig. 1. Block diagram of the experimental apparatus.

with a resonance frequency close to 1 MHz. The AE signals detected by the sensor were amplified by a charge amplifier of 60 dB and a main amplifier of 10 dB. These amplified signals were, after conversion from analogue to digital signals, classified into eight levels of amplitude (0·2, 0·4, 0·6, 0·8, 1·0, 1·25, 1·5 and 2·0 V) by a pulse-height histogrammer, and then accumulated at every one-second interval. The numbers of the AE signals in eight different levels were printed out. In this experiment, the gain of the overall system was 70 dB and the threshold was set at 0·15 V.

In general, the AE waveform can be regarded as a typical damped wave and the energy of the AE signal is known to be closely related to the fracture process. For the evaluation of the AE energy, two methods have been proposed;[5] a square of the maximum amplitude and an integrated area of the waveform. In this experiment, the former method was adopted, and the energy of the AE wave (E_{AE}) was evaluated by the square of the maximum AE amplitude (V_{o-p}).

3 Results

3.1 Fracture behavior and AE characteristics

All of the experimental results on crack extension and AE signals are shown by overlapping on the load–COD curves of the samples A, B and C in Figs 2, 3 and 4, respectively. In these figures, an event in acoustic emission is indicated by an open symbol at each level of amplitude.

The load–COD curves of the three samples show non-linear behavior from the early stage of loading until fracture. Therefore, the fracture toughness of the samples can not be estimated by linear elastic

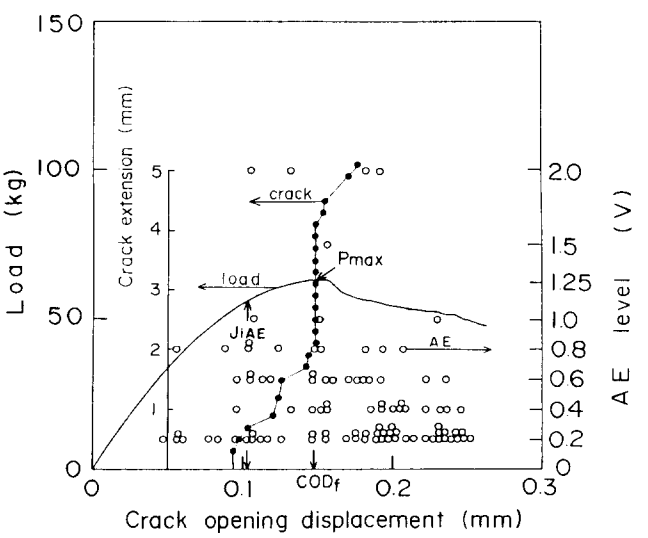

Fig. 2. AE in fracture toughness test for the sample A.

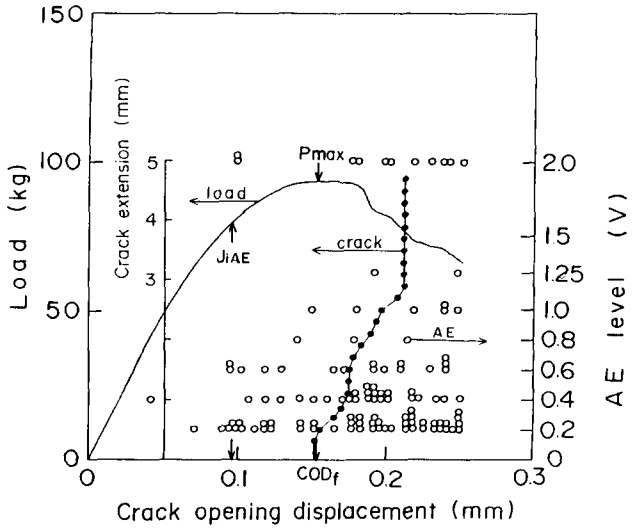

Fig. 3. AE in fracture toughness test for the sample B.

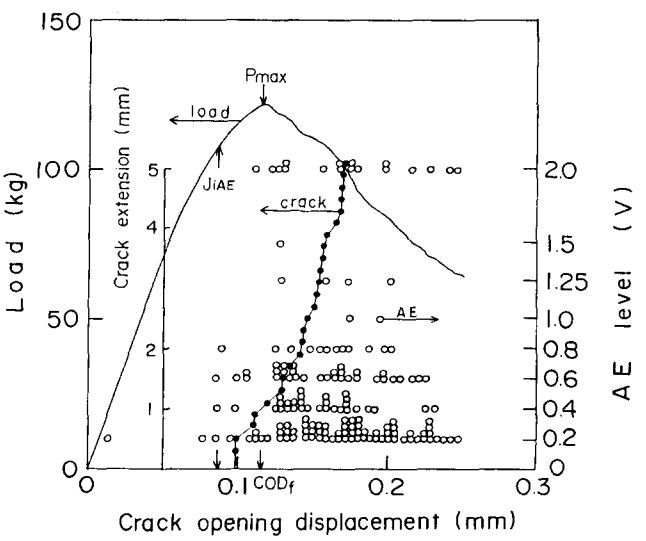

Fig. 4. AE in fracture toughness test for the sample C.

fracture mechanics. In a previous report,[1] the same fracture behavior was observed and it has been already concluded that the J-integral was suitable for the evaluation of the fracture toughness of electrode materials according to ASTM E-399. Hence the J-value is adopted for the evaluation of fracture toughness in this experiment.

As shown in the figures, the COD-value which corresponds to each maximum load (COD_f) tends to vary with Young's modulus; sample C having the highest Young's modulus, showing the highest maximum load, P_{max}, and the smallest COD_f. Since the maximum point of the load–COD curve cannot be decided clearly, the shape of the load–COD curves around the maximum point was approximated roughly by Gaussian distribution and the positions of COD_f were decided as shown in each figure by arrows.

The macroscopic crack extension detected by the crack gage is also plotted by filled symbols in the same figures. In sample A, the crack starts to grow even at a low load, much lower than the maximum load, P_{max}. In the samples B and C, on the other hand, the initiation of macroscopic crack is observed near the maximum load.

In sample A, with the lowest Young's modulus, AE signals are already detected at one-third of COD_f. At two-thirds of COD_f, which corresponds to the load of 80% of the maximum, the signals at high levels above 2·0V occur suddenly. On the other hand, sample C, with the highest Young's modulus, represents the latest initiation of low-level and high-level (above 2·0V) signals near COD_f and continues to generate the high-level signals in spite of the decrease of load.

The numbers of AE signals detected at each energy level before reaching the macroscopic crack extension up to 5 mm by crack gage are shown in Table 2. It is clear that the sample with high Young's modulus gives a high number of monitored AE signals at each AE level. The following tendency is seen; the artificial graphite electrode with high Young's modulus gives late initiation of AE signals, but a large number of the signals.

3.2 Determination of J_{iAE}

In Fig. 5, the cumulative sum of AE wave energy ($\sum E_{AE}$) is plotted against J-value. On each sample, a stepwise increase in $\sum E_{AE}$ is observed. The J-value corresponding to this jump in $\sum E_{AE}$ is reasonably assumed to be a critical one for the initiation of macroscopic crack growth. This critical value in J is usually expressed as J_{IC}, but in this experiment is denoted as J_{iAE} because it is determined from AE data. In sample A, the second abrupt increase is

Table 2. Histogram of AE energy levels up to 5 mm (crack gage)

Electrode	*Histogram of AE energy level (V)*								
	0·2–0·4	*0·4–0·6*	*0·6–0·8*	*0·8–1·0*	*1·0–1·25*	*1·25–1·5*	*1·5–2·0*	*2·0–*	*Total*
A	20	6	11	7	2	0	1	2	49
B	30	20	12	2	2	1	0	6	73
C	39	21	20	8	1	2	1	8	100

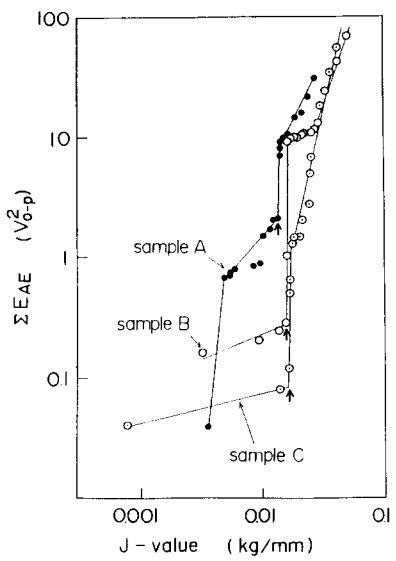

Fig. 5. $\sum E_{AE}$ versus J-value for the samples A, B and C. The arrows show the J_{iAE}-value for each sample.

adopted, because the first one is caused by only one event at the 0·8 V level, which is reasonably assumed to be noise from outside of the system. The J_{iAE}-values of the samples A, B and C determined in Fig. 5 are 0·0135, 0·0155 and 0·0165 kg/mm, respectively.

These J_{iAE}-values are shown in Figs 2, 3 and 4 as arrows on the load–COD curves, which correspond reasonably to the first occurrence of high-level AE signals in each sample. The load corresponding to the J_{iAE}-value is in the range of 85 to 90% of the maximum load P_{max}. The COD corresponding to the J_{iAE}-value shows a similar value of about 0·1 mm and does not coincide in position with COD_f on each sample. The relative position of the J_{iAE}-value to the macroscopic crack extension detected by a crack gage differs in the three samples used.

The relation between J_{iAE} and Young's modulus is shown in Fig. 6. The sample with a high Young's modulus has a high value of J_{iAE}, that is high fracture toughness.

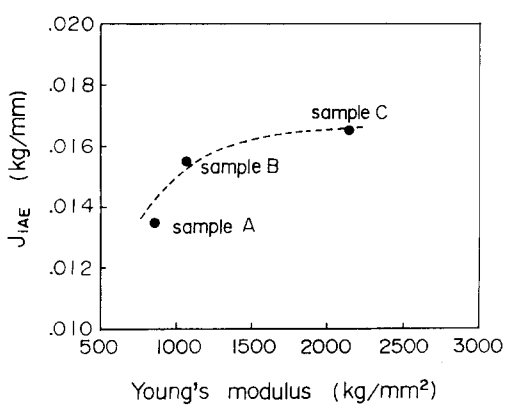

Fig. 6. J_{iAE} versus Young's modulus for the samples A, B and C.

4 Discussion

4.1 Fracture behavior and macroscopic crack initiation

Slagle[6] and Sakai *et al.*[7] have reported the following scheme of fracture behavior on polycrystalline graphite containing many pores. A number of microcracks generate from the early stage of loading at the tips of the notch introduced and also of the pre-existing pores. The further loading leads to the extension and widening of microcracks. Finally, the failure occurs when these microcracks join together to make a macroscopic crack and form a fracture path. Most microcracks remained closed after stress release.

The fracture behaviour of the artificial graphite electrodes used in this experiment seemed to follow this general scheme. The load–COD relations observed on three samples showed non-linear behavior and the signals of the low energy level were detected from the early stage of loading. Therefore, the departure from elastic relation was supposed to be caused mainly by microcracking. It seemed to be remarkable in the case of graphite materials because they contain a large amount of pre-existing pores.

Before reaching the maximum load P_{max} an abrupt increase in AE energy was observed by analyzing AE signals detected and more clearly by using cumulative AE wave energy, which seemed to correspond to a moment of macroscopic crack initiation. Therefore, the J-values determined from the abrupt increase in cumulative AE energy, J_{iAE}, could be considered to be the critical value for the initiation of macroscopic crack, J_{IC}. The J_{iAE}-values determined in this experiment on three graphite electrodes were in the range of 0·0135 to 0·0165 kg/mm, which were a little higher than those reported on high-density isotropic graphites.[8] The COD-values giving J_{iAE}-values are indicated in Figs 2 to 4; their positions relative to the COD_f-values are roughly the same. It has been pointed out already by direct observation that macroscopic cracks start to propagate even before reaching P_{max} and COD_f.[6]

The crack extension detected by a crack gage increased gradually even in the early stage of loading because of the introduction of microcracks at the tips of pre-existing pores. It showed also a jump at certain COD-values, but its relative position to COD_f scattered on three samples; around the COD_f-value in sample A, but far above the COD_f-values in samples B and C. These abrupt increases of crack extension gave extremely high values of J_{IC}, which seemed to be unreasonable. It seemed to be unreasonable that in sample B the crack extension was

detected by the crack gage to start around COD_f and its jump occurred far behind COD_f.

Previously the increase of electrical potential was measured during the fracture toughness test and it was attempted to relate this to macroscopic crack initiation. The potential increased gradually in the early stage of loading mainly due to microcracking, but neither a clear turning point nor abrupt increase in potential was observed.[1]

In conclusion, the AE method to detect the initiation of macroscopic crack and consequently to determine J_{IC}-value is effective, in comparison with the measurements of crack extension by using crack gages and by measurement of electrical potential increase. However, it might be necessary to carry out more precise and well-focused comparison among these techniques to detect macroscopic crack initiation.

4.2 AE generating model of porous graphite

On the basis of the present experiment, the following model for AE generation in porous graphite materials is proposed. As schematically shown in Fig. 7(a), the artificial graphite electrode is considered to be composed of coke particles with different sizes and a matrix derived from coal-tar pitch binder. There are many pores in the coke particles, in the matrix derived from the binder, and also at the interface between the matrix and the coke particles. Even at a low level of loading on this porous material, a few microcracks initiate from the tips of the induced notch and pre-existing pores in the vicinity of the concentrated stress area, as shown in Fig. 7(b). This microcracking is reasonably assumed to generate low-level AE signals and also to cause the slight departure from elastic deformation, as observed in this experiment. By further loading, the microcracks tend to increase their length and width, and finally to join together to make some macroscopic cracks (Fig. 7(c)). At this moment, high amounts of energy are consumed at several positions in the process zone and consequently AE signals with high energy levels are emitted. This high energy consumption seems to correspond to a jump in cumulative AE wave energy. In graphite materials, a macroscopic crack extends gradually by associating the microcracks formed, which causes a complicated fracture path and remarkable branching of the crack. This seems to be the reason why the high-level AE signals are detected even after the initiation of macroscopic crack and also why the load is maintained in rather high values even after exceeding the COD_f.

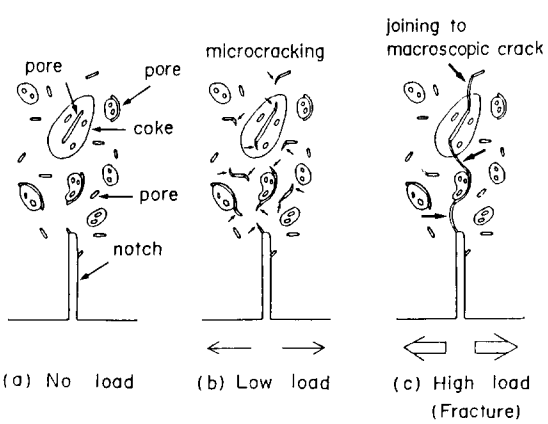

Fig. 7. AE signal generating model.

References

1. Ekinaga, N., Three-point bending fracture toughness test of artificial graphite electrodes by electrical potential method. *TANSO*, **114** (1983) 97–102.
2. Takahashi, H., Niitsuma, H., Suzuki, M. & Mori, Y., Classification of AE behavior in fracture toughness test and its fracture mechanics evaluation. *J. Non-Destructive Inspection*, **30** (1981) 890–5.
3. Niitsuma, H., Takahashi, H. & Chubachi, N., Frequency analysis characterization of AE behavior and microfracture process. *J. Non-Destructive Inspection*, **30** (1981) 903–10.
4. Standard method of test for elastic–plastic fracture toughness J_{IC}. The Japan Society of Mechanical Engineers, JSME Standard S 001, 1981.
5. Kishi, T. & Kuribayashi, K., Material evaluation by acoustic emission. *Bull. Japan. Instit. Metals*, **20** (1981) 167–75.
6. Slagle, O. D., Deformation mechanics in polycrystalline graphite. *J. Am. Ceram. Soc.*, **50** (1967) 495–500.
7. Sakai, M., Yoshimura, J., Goto, Y. & Inagaki, M., R-Curve behavior of a polycrystalline graphite: Microcracking and grain bridging in the wake region. *J. Am. Ceram. Soc.*, **71** (1988) 609–16.
8. Oku, T., Ishiyama, S., Takahashi, H., Fukazawa, T. & Hashida, T., An evaluation of fracture toughness of graphites for high-temperature gas-cooled reactors by the ISRM core testing method used jointly with AE method. *TANSO*, **139** (1989) 175–81.